

Rapid Prototyping Assisted Scaffold Fabrication for Bone Tissue Regeneration

Pranav S. Sapkal¹, Shraddha Jaiswal¹ & Abhaykumar M. Kuthe¹

¹ Department of Mechanical Engineering, Visvesvaraya National Institute of Technology, Nagpur, India

Correspondence: Pranav S. Sapkal, Department of Mechanical Engineering, Visvesvaraya National Institute of Technology, Nagpur, India. E-mail: pranav_sapkal@rediffmail.com

Received: August 27, 2016

Accepted: September 26, 2016

Online Published: September 30, 2016

doi:10.5539/jmsr.v5n4p79

URL: <http://dx.doi.org/10.5539/jmsr.v5n4p79>

Abstract

The review article focuses on Rapid Prototyped assisted scaffold fabrication for bone tissue regeneration, particularly in respect of its mechanical properties and cell culture abilities. The distinct feature of computer aided design and computer aided manufacturing (CAD & CAM), imaging technology and rapid prototyping (RP) technology has been used by different researchers to print porous scaffolds with requisite shape and interconnected channels for osseous tissue formation. This study concludes that the use of RP in scaffold manufacturing offers patient specific designed scaffolds with improved strength, in-vitro and in-vivo cell culture capability unlike traditional scaffold fabrication techniques. Tissue engineering using 3D Printing is a viable substitute for organ transplant, which requires willing donors to part with their organs. This study reviewed the benefits of RP/imaging/CAD-CAM to develop scaffolds for bone tissue regeneration and it serves those patients who could not be accurately treated by traditional means. The article is helpful to study the influence of RP in the field of organ transplant

Keywords: Rapid prototyping (RP), Fused Deposition Modeling (FDM), Low-Temperature Deposition Manufacturing (LDM), Computer aided design/Computer aided manufacturing (CAD/CAM), Mesenchymal stem cells (MSC), Microstereolithography (MSTL), Tissue engineering (TE)

1. Introduction

Hard tissue structure comprises of cortical and cancellous bone. Cortical bone is closely packed sharing 80% of the whole bone mass while remaining 20% is shared by cancellous part. Remodeling and maintenance of bone is carried out by different cells. Osteoblast cell is responsible for bone generation, whereas the function of Osteoclast cell is bone resorption. The communication among different cells (Osteocyte, Osteoblast and Osteoclast) together is responsible for maintaining healthy bone (Bose, Vahabzadeh, & Bandyopadhyay, 2013). However body fails to completely cure large size, bone defects (Mourino & Boccaccini, 2010).

Existing medical solutions for functional substitution of these crucially injured or diseased bones are medical implants and organ transplantation (Yang et al., 2001). However, problems associated with these solutions like chronic infection, irritation and dislocation from the site compels us to find new alternatives. Tissue engineering an emerging field involves the generation of new tissues by using the principles and methods of engineering and cell culture. In this technology cells from the patient's own body are expanded in-vitro and are then seeded on a scaffold which channelizes the growth of cells in predefined orientation to form three dimensional tissues (Sun & Lal, 2000; Sachlos & Czernuszka, 2003).

Traditional approaches to fabricate these scaffolds are gas foaming, particulate leaching, fiber bonding, phase separation, membrane lamination, melt molding, solvent casting and emulsion freeze drying (Zein et al., 2001). But these scaffold fabrication methods do not provide desired inner architecture that makes sure biological process and tissue establishment (Chen et al., 2005). Such intricate structures can be successfully fabricated by additive manufacturing (AM) techniques. Some major techniques involve, Three Dimensional Printing (3DP), Stereo lithography (SLA), Fused Deposition Modeling (FDM), Selective Laser Sintering (SLS), 3D Plotter, Phase-change Jet Printing and Low Temperature Deposition Manufacturing (LDM) that let fabricate difficult inner structures directly from CAD data (Landers et al., 2002).

The achievement of cell proliferation on scaffold depends on various parameters like its porosity, surface area to volume ratio, strut/wall thickness, anisotropy, cross sectional area, permeability and interconnected porosity. A perfect scaffold should have interconnected macro pores in the range of 100 to 350 μm for good release of oxygen and nutrients and micro pores on the scaffold surface in the range of 5 to 10 μm for initial cell adhesion (Kalita, Bose, Hosick, & Bandyopadhyay, 2003; Hutmacher, Sittinger, & Risbud, 2004).

Apart from cell performance, mechanical properties of scaffold play a primary role in load bearing sites. Several studies are based on optimizing the porosity value of scaffold with compressive modulus of the host tissue (Sun, Starly, Darling, & Gomez, 2004; Rainer et al., 2011). However, some studies say that there is no need to match the mechanical properties of scaffold with the host tissue since the implant is intended to get remodeled and would be replaced by bone (Fedorovich et al., 2011). The main aim of the paper is to provide various research activities carried out on rapid prototyping (RP) assisted fabrication of scaffold for the osseous tissue formation. The paper is divided into 5 sections. Section 2 talks about the CAD based approaches that are used for designing patient specific scaffold architecture and its further printing using rapid prototyping technology. Section 3 speaks about the increase in mechanical properties of the scaffolds fabricated using a rapid prototyping approach than that of traditional approaches. Cell culture abilities of 3D-printed scaffold and its comparison with that of conventional fabricated methods is discussed in section 4. Section 5 describes the animal studies that are carried out on 3D printed scaffolds for bone tissue regeneration.

2. Computer Assisted Scaffold Architectures for Bone Tissue Regeneration

A lot of development has taken place in scaffold architecture as far as bone tissue engineering is concerned. Since traditional methods of scaffold fabrication did not prove to be efficient in terms of its mechanical and cell culture abilities, CAD based scaffold design led researchers to fabricate scaffold with required shape and size. Chua et al. (2003) worked on the development of library with diverse polyhedral shapes to form the unit element of the scaffold structure. In Part1 of his paper the unit cells were chosen based on their complexity, mechanical integrity, gap filling properties and assembly of such unit cells was chosen to form a scaffold structure. Whereas in Part2 a program is made to automate the assembly of selected polyhedral unit cells to form the scaffold structure of required outline and dimension Figure 1 (Chua et al., 2003a,b). Another well-known approach to get patient specific scaffold is a Boolean intersection of scaffold unit cell and host tissue anatomic structure Figure 2 (Sun, Starly, & Darling, 2005). In another study wire frame estimation of basic polyhedral, the platonic solid and Archimedean was used. Each edge of the model is converted to a beam of desired length. By changing the diameter of the beam porosity of 80% is maintained, a value close to the porosity of trabecular bone. Assembly of such unit elements forms the scaffold structure for bone regeneration (Wettergreen et al., 2005).

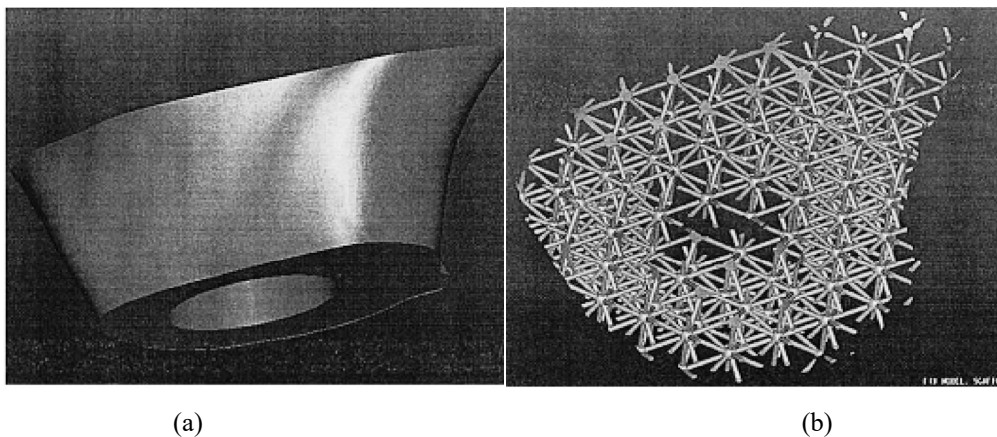


Figure 1. (a) Reconstructed surface model; (b) Scaffold assembly ready for RP fabrication (Chua et al., 2003b)

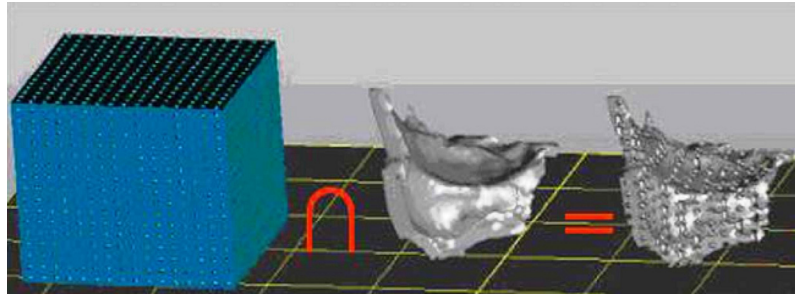


Figure 2. An example of using Boolean operators to achieve bone scaffold anatomical geometry (Sun, Starly, & Darling, 2005)

CAD based scaffold design with various porosities obtained by changing FDM parameters like road width, slice thickness, angle between two successive layers and road gap, 3D honeycomb pattern is obtained, also novel architectures replicating human bone with a gradient in porosity levels for cortical and cancellous bone is reported by Kalita et al., 2003 Figure 3 (Kalita, Bose, Hosick, & Bandyopadhyay, 2003). Porous scaffold for bone tissue repair is reported by Liulan et al. (2006), in which firstly CAD model with essential interior microstructure is created and Boolean subtraction of the scaffold bounding box and the model is done to get the requisite negative model of casting mold. FDM an additive manufacturing technology, which uses the ABS as model material is used to print this mold. Ceramic slurry of β -tricalcium phosphate (β -TCP) is poured into the mold and subjected to necessary temperature conditions. By melting the ABS mold and sintering the β -tricalcium phosphate powder scaffold with required internal structure is obtained Figure 4 (Lin et al., 2006). In an additional study by the same researcher, scaffold fabrication by using SLS (Selective Laser Sintering) an additive manufacturing technology in which the unit element consists of microstructure of spheres. The intersection of the two spheres is in such a fashion, so as to achieve desired interconnected porosity. This unit microstructure is repeated in x, y, and z direction to get three dimensional pattern. The final scaffold structure is obtained by performing Boolean subtraction between solid cubic model and three dimensional microstructure patterns (Liulan, Qingxi, Xianxu, & Gaochun, 2007).

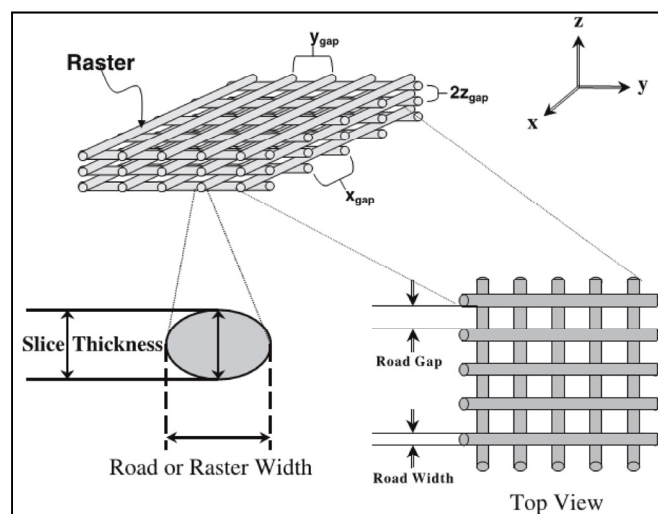


Figure 3. Schematic of internal architecture of a porous prototype with 3-D interconnectivity showing all the important FDM processing parameters associated with the design and development (Kalita, Bose, Hosick, & Bandyopadhyay, 2003)

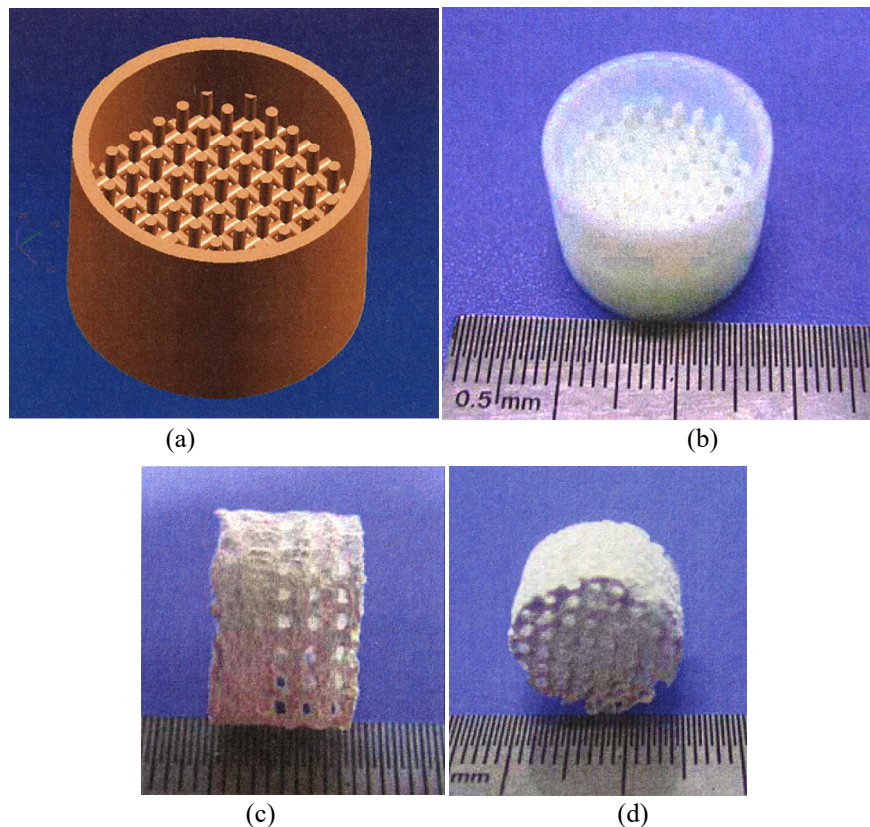


Figure 4. (a) The CAD model of scaffold. (b) ABS, casting mold. (c) The side elevation of the bioceramic scaffold. (d) The planform of the bioceramic scaffold (Lin et al., 2006)

Using the finite element method, scaffold based on conformal all-hexahedral mesh refinement and shape function is investigated by (CAI and Xi, 2008; Hu, 2012). Scaffold exterior model, including the cortical bone and cancellous bone is created by taking the CT scan of the region of interest. Based on a grip mapping algorithm the scaffold model is meshed by eight -node hexahedral element since it enjoys easy control than twenty-node element. The mesh is further refined so as to obtain controlled pore size distribution at different location of the scaffold. By getting the node information of the hexahedral element, pore making element is modeled for all 3D hexahedral mesh. Boolean subtraction operation between the scaffold exterior model and pore model is performed to get the scaffold with defined pore size distribution Figure 5 (Cai & Xi, 2008; Li et al., 2012).

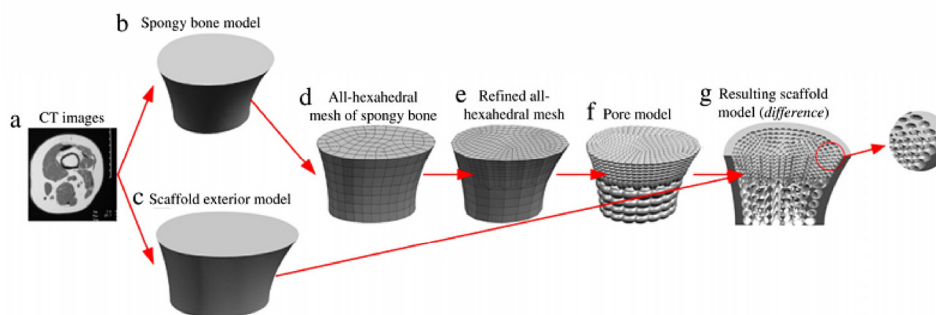


Figure 5. Scaffold with varying porosity using hexahedral mesh refinement (Cai & Xi, 2008)

Different cell fate processes such as cell replication, cell differentiation, cell death, cell motion and cell adhesion predominantly depends upon scaffold material and architecture. Most of the studies are based on scaffold

fabrication with pore sizes ranging from 150-300 μm and 500-710 μm to facilitate osseous tissue formation (Li et al., 2006). However, there is no agreement among researchers in respect of best pore size for bone regeneration. Scaffold fabricated from Poly (propylene fumarate) a biodegradable photopolymer using microstereolithography showed an increase in pre-osteoblast cell proliferation with an increase in pore size for 100, 200 and 350 μm but exhibited discouraging results with 500 μm pore size because of lesser initial cell bond with the scaffold (Lee, Ahn, Kim, & Cho, 2010). Scaffold with same overall porosity and pore size but with different architecture also shows variation in cell proliferation. Not only pore size, but scaffold architecture and porosity also play an important role in enhancing the cell reaction in terms of seeding efficiency. Poly (ϵ -caprolactone) (PCL) scaffold with four different configurations of fibers (basic, basic-offset, crossed and crossed offset) each having mean porosities of about 60% showed more cell propagation and mesenchymal stem cell differentiation in offset structures when seeded with rat bone marrow (MSC) (Maleksaeedi et al., 2013). Scaffold fabricated by PPF using Microstereolithography (MSTL) an additive manufacturing technology showed 30% more cell proliferation for staggered structure than lattice type when seeded with pre-osteoblast cells (Lee, Ahn, Kim, & Cho, 2010).

Scaffold architecture also has to be designed keeping in mind the fluid flow inside it in a bioreactor. Diameter of scaffold strand, distance between the two strands and fluid flow through the scaffold affects the distribution of shear stress in a perfusion bioreactor. A study carried out by Yan et. Al., (2011) in which fluid flow in both perfusion and non-perfusion is modeled in computational fluid dynamics (CFD) environment and shear stresses at the surface of the scaffold were computed. It was seen that the shear stress value increased with the increase in the strand diameter in perfusion bioreactor and is very high as compared to non-perfusion and hence it detached the cells from the surface of the scaffold and cell growth is hampered (Yan, Chen, & Bergstrom, 2011). Distribution of cells after perfusion seeding in a tissue engineered scaffold is influenced by its pore architecture. In a study carried out by Melchels et al. (2011) in which two scaffold type one with homogeneous pore size ($412 \pm 13 \mu\text{m}$) and porosity ($62 \pm 1\%$) and another with varying pore size (250-500 μm) and porosity of (35%-85%) were modeled. Computational fluid dynamics results revealed that their was unvarying flow of fluid velocities and wall shear rates of ($15\text{-}24\text{s}^{-1}$) for homogeneous structure, whereas for varying structure their was different in the fluid velocities and wall shear rates from 12 to 38s^{-1} . Greater cell densities were seen in scaffold with larger pores in gradient architecture since with a larger pore size, number of cells are passing through it in a unit time is more as compared to smaller pores (Melchels et al., 2011). Micro - scale scaffold based on actual CT images of patients is reported by Podshivalov et al. (2013). The scaffold manufactured by state-of-the-art 3D an additive manufacturing technology showed very alike structure as that of host tissue and hence good interaction with the surrounding tissue. By taking the μCT images of the host tissue, 3D model of region of interest is constructed. By converting the 3D volumetric model into 3D scaffold design, FEA analysis is done in order to find the weaker sections. Finally the model is converted into the .STL file format and directly sent to additive manufacturing. Scaffold geometry verification is done by taking the μCT again and is dispatched for implantation (Podshivalov et al., 201).

3. Mechanical Testing of 3D Printed Scaffold for Bone Tissue Regeneration.

Mechanical properties of scaffold have a leading role when regenerating firm tissues like bones and cartilages (Chua et al., 2003a,b). It should provide enough mechanical strength for early injury contraction forces and later modeling of the tissue (Hutmacher, Sittinger, & Risbud, 2004). Degradation of scaffold material hampers its mechanical strength and hence the degradation rate should match the regeneration rate (Sun, Starly, Darling, & Gomez, 2004). Scaffold with high degradation rate should have low porosity level since fast degradation will lessen the structural strength. Whereas scaffold with low degradation rate and good mechanical properties can have high porosity values, since with larger pores cell interaction and multiplication will enhance (Karageorgiou & Kaplan, 2005).

Intricate CAD based scaffold architectures and its pre deterministic mechanical simulation is not possible with traditional approaches. RP assisted scaffold fabrication has led researchers to fabricate scaffold with different architectures in order to enhance the mechanical properties of the same material with same porosity levels. Finite element analysis of unit polyhedral shapes modeled in CAD environment with same overall porosity of 80 %, bounded by same dimensions with difference in its architectural arrangements showed variation in its elastic modulus of 174 MPa for an element with (square hole) and 0.96 MPa for the element (curved connector) when the elements were subjected to 1% strain (Wettergreen et al., 2005). Another study by Sun et al. (2004) has reflected a FEM approach to optimize the design of the unit element of scaffold. Unit cubic elements with square holes from each side were modeled in CAD environment with varying porosity levels. By fixing one face of the cubic element and giving a displacement of 0.1 % of the length, reaction force at the fixed end is computed and elastic modulus for respective element is calculated. Three different materials viz. hydroxyapatite, PLLA and PLGA were analyzed. Since minimum porosity of 60 % is required for efficient nutrient transport, material element with 60% porosity is selected which satisfies the elastic modulus property of the host tissue (Sun, Starly, Darling, & Gomez, 2004).

FDM approach has been used by researchers to fabricate polymer, ceramic as well as polymer-ceramic composite scaffold. PP (polypropylene) – TCP scaffold with 3-D interconnected controlled porosity fabricated using FDM approach has been reported by Kalita et al. (2003). Porous structures were fabricated by processing the filament using a single screw extruder followed by its deposition in fused form. A scaffold structure with a pore size of 160 μm and total porosity of 36, 40 and 52 % were fabricated. Compression test results demonstrated that structure with 36% porosity level revealed the best compressive strength value of 12.7 MPa which is well in range for human trabecular bone (Kalita, Bose, Hosick, & Bandyopadhyay, 2003). Bioinspired approach for the fabrication of load adaptive scaffold architecture with same porosity level, nevertheless with different architecture is also stated by Rainer et al. (2011). PCL poly (e-caprolactone) a biodegradable polymer is used to print two different architectures, one designed with load adaptive scaffold architecturing (LASA) and another with the grid design (linear strut alternately oriented at 0 and 90⁰) Figure 6. Both the structures were designed with 61 % porosity levels. Samples were compressed with a rate of 1mm/min and load vs. displacement graph was plotted. The stiffness value of LASA structure obtained was 5.50×10^5 N/m where as for GRID structure; it was 1.40×10^5 N/m (Rainer et al., 2011).

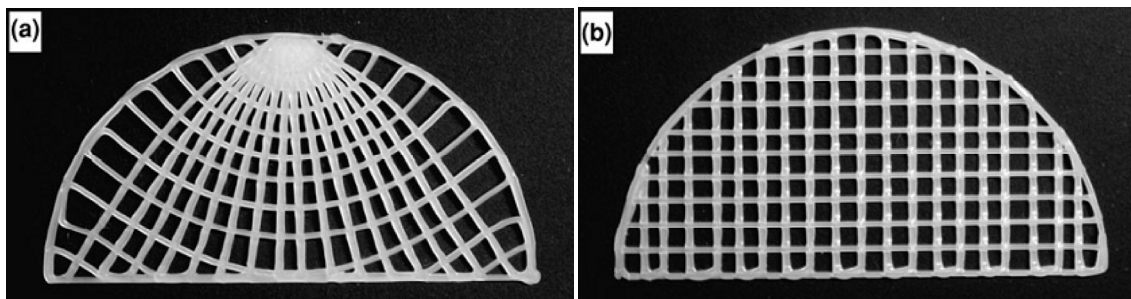


Figure 6. Poly (e-caprolactone) structures produced according to the LASA (a) and GRID (b) models (Rainer et al., 2011)

Studies in different fabricating process of the scaffold and its effects on mechanical properties have also been reported. Scaffold fabricated using traditional approach like salt leaching and with that of microstereolithography (MSTL) using Poly (propylenefumarate) a biodegradable photopolymer has been compared for its mechanical and cell proliferation abilities. It was observed that scaffold fabricated using salt leaching method showed average values of ultimate strength and elastic modulus of 1.29 and 15.49 MPa, whereas there was significant increase in values i.e. 8.28 and 77.41 MPa for scaffold fabricated using MSTL approach (Lee, Ahn, Kim, & Cho, 2010).

Selective laser sintering technology is successful for the fabrication of scaffold with polymer, ceramic as well as metallic material. PCL a bioresorbable polymer has been used in scaffold fabrication as far as bone generation is concerned. In a study carried out by Williams et al. (2005) in which PCL scaffold fabricated by SLS technology for pig condyle showed compressive modulus of 52 to 67 MPa and yield strength of 2.0 to 3.2 MPa, which is very much close to the properties of human trabecular bone (Williams et al., 2005). Silicate/Hydroxyapatite (HA) hollow composite ceramic scaffold manufactured for bone tissue engineering using selective laser sintering is confirmed by Liu, F. (2012) in his study. Silica sol 23 weight % embedded with 40 weight % HA particles and water, was used to make ceramic slurry. The maximum bending strength of 4.7 MPa was obtained when the slurry was processed with 1.6 J/mm² laser energy to form the green body and then sintered at 1200⁰C for 1.5 hours (Liu, 2012). Liu et al. (2013) have again investigated the use of titanium and silica sol slurry for the fabrication of hollow bone scaffold using SLS and found that the compressive strength of 142 MPa was achieved after sintering the green part at 900⁰C for 2 hrs (Liu et al., 2013).

Patient specific scaffold produced by 3D –printing technology directly by using CT data is probed by many researchers. CT data of anonymous patient's left hand were acquired and its 3-D model was created in a CAD environment. Region of interest, i.e. left hand's ring finger proximal phalange was used for the case study. The model was directly sent to the 3-D printer and binder was printed layer by layer on beta tri-calcium phosphate powder bed. The printed model was subjected to high temperature treatments so as to increase its mechanical strength. It was observed that the compressive strength values increased from 2.36 MPa for sintering temperature of 1250⁰C to 8.66 MPa when sintered at 1400⁰C (Santos et al., 2012). Superior mechanical properties of scaffold have also been achieved using 3-D printing technology. Titanium powder and PVA (Polyvinyl alcohol) a water soluble polymer was dry mixed in a ball mill using 20 mm zirconium balls for 10 hrs. The mixed powder was laid

on the bed which was controlled by a feed roller and deionized water which was used as a binder was dispersed by the printer head layer by layer according to the cross section of scaffold. Compressive modulus of 330 MPa was obtained for total scaffold porosity of 83 %, which is well in range for human cancellous bone (Maleksaeedi et al., 2013). Table 1 summarizes the mechanical properties of scaffold fabricated by additive manufacturing technology for bone tissue engineering.

Table 1. Mechanical testing of 3D printed scaffold for bone tissue regeneration

Material	Technique	Average Porosity %	Application	Compressive Modulus (MPa)	Compressive Strength (MPa)	Compressive Yield strength (MPa)	Stiffness (N/m)	Bending Strength (MPa)	References
PP-T CP	FDM	36		264 ± 28.6	10.4 ± 1.2				Kalita et al., 2003
HA	FEM	60	Femoral head	673.4					Sun et al., 2004
PLLA	Analysis			909					
PLGA				1380					
PCL	SLS	63 to 79%	Pig condyle	52 to 67		2.0 to 3.2			Williams et al., 2005
β-T CP	FDM (Indirect method)	63.4	Cambium (Bone repair)			0.745			Williams et al., 2005
PCL	3D- Plotter	53	Bone tissue regeneration	10.39		4.1			Hee et al., 2010
PPF	MSTL	69.6	Bone tissue regeneration	77.41		8.28			Melchels et al., 2011
PLGA	3D-printer	50 70	Human trabecular bone	321.6 ± 140.9 89.5 ± 36.8		10.3 ± 4.3 2.1 ± 1.2			Saito et al., 2010
PLGA + T CP	LDM	87.5	Alveolar bone	67.87		1.37			Li et al., 2011
PCL	FDM	61	Femoral head				5.5 x 10 ⁵		Rainer et al., 2011
Silica + HA	SLS	27 – 30	Bone tissue regeneration					2.2 – 4.77	Liu, 2012
PCL + HA HA – 40%	FDM	54.6 ± 1.2	Goat femoral head	57.90 ± 5.70	4.2				Ding et al., 2013
PCL	3D- Bioplotter	60	Bone tissue regeneration	18.5 ± 0.19					Yilgor et al., 2008
β-T CP	3D Printing	54.44±2.03 53.19± 1.19 50.85±2.26 46.07±8.52	Left hand's Ring finger proximal phalange		2.36 ± 0.05 5.75 ± 0.05 8.30 ± 0.14 8.66 ± 0.11				Santos et al., 2012
Glass- Ceramic	SLS	61	Bone tissue regeneration		12.37 ± 1.25				Li et al., 2013
PLLA	PEM	60.3	Bone tissue regeneration	194.96		8.32		20.33	Xiong et al., 2001
PLLA + T CP	LDM	89.6	Bone tissue regeneration	60.11		4.71		12.10	Xiong et al., 2002
Titanium	SLS		Bone tissue regeneration		142				Liu et al., 2013
Titanium	3D-printing		Bone tissue regeneration		2090				Maleksaeedi et al., 2013

4. In-vitro Studies

4.1 in-vitro Studies Carried Out on Scaffold Fabricated via Additive Manufacturing Technology.

Many studies are reported for scaffold fabricated by 3D-printing technology using Mesenchymal stem cells for in-vitro evaluation. MSC's which are undifferentiated cell from an embryo, fetus and adult with high proliferation and self-renewal ability that under certain conditions can differentiate into multiline age specialized cells (Lian et

al., 2014). Mesenchymal stem cell can be derived from Bone marrow (BM-M SCs), adipose tissue (AT-MSCs), peripheral blood (PB-MSCs), the lungs or heart, dental pulp, skeletal muscles etc. using different scientific protocols (Hass, Kasper, Böhm, & Jacobs, 2011). Immunofluorescence study and WST assay to examine cell morphology and adhesion on PLA based composite scaffold fabricated by 3D-printing using rat mesenchymal stem cells (rMSC) derived from bone marrow has been studied by Serra et al. (2013). Two different material compositions: a) PLA/PEG (Polyethylene glycol), and b) PEG and G5 (CaP glass) glass particles combined with PLA matrix were printed layer by layer using the nozzle deposition system. It was revealed by WST assay that there was no noteworthy difference in the absorbance value for both the compositions, when incubated for 4 hrs. However immunofluorescence studies demonstrated that there was a momentous difference in cell morphologies for both the scaffold. PLA/PGE scaffold showed the very sparse distribution of rMSC and the cells were mostly round in shape, whereas there was very well spread morphology of rMSC for scaffold with glass particle (Serra, Planell, & Navarro, 2013).

Compared with other sources adipose tissue has more population of MSCs and it is easy to harvest (Locke, Windsor, & Dunbar, 2008). About 1g of adipose tissue yields 5000 AT-MSCs (Levi & Longaker, 2011). They are expanded *in vitro* and evaluated *in vivo* for cartilage and bone formation which represents an attractive source of cells for bone Tissue Engineering (Aust et al., 2004). The effect of osteogenic differentiation of adipose derived mesenchymal stem cells in the 3-D printed polycaprolactone scaffold is studied by Caetano, G. F. (2015). To evaluate the ADSC's viability on PCL scaffold cultured in both (basic and osteogenic medium), the MTT colorimetric assay test was performed. Macroscopic images of scaffold showed that purple formazan crystals were formed because of the mitochondrial activity as a result of presence of viable cells. The purple crystals formed on the scaffold were dissolved in DMSO and optical density (OD) values of the solution were recorded using a spectrophotometer. It was observed that OD values for both the groups (basic and osteogenic) medium showed similar results (Caetano et al., 2015).

Embryonic Stem Cells demonstrate potential for application in the field of regenerative medicine (Marolta et al., 2012). They are derived from blastocyst-stage of the embryo. ESCs are prone to genetic alterations and can develop abnormal karyotype; therefore close check on karyotype is recommended (Colnot, 2011). NIH3T3 mouse fibroblast cell line extracted from embryo has been used to see the cell attachment and proliferation on PELA (poly (D, L-lactic acid) - poly (ethylene glycol) - poly (D, L-lactic acid) and HA/PELA composite scaffold fabricated using FDM approach. CCK-8 assay revealed that initial cell attachment was higher for HA/PELA scaffold than that of PELA, and much higher live cells were observed in HA/PELA scaffold for 14 days. Whereas much lower cell attachment for PELA resulted in cell necrosis by day 3. The cell attachment difference was again confirmed by Formosan die. HA/PELA scaffold sustained the attachment of live cells and were well dispersed along the layers of scaffold, whereas in PELA scaffold, very less number of live cells were trapped between the pores. Further, to assess the potential of HA/PELA scaffold for osteogenic differentiation of rMSCs, the scaffolds were cultured with osteogenic and expansion media for 14 days. The result displayed phosphate staining all over the 3-D macropores which confirmed osteogenic differentiation of rat mesenchymal stem cells in osteogenic media (Kutikov, Gurijala, & Song, 2014).

Tissue specific osteoblast cells have been used in many studies to evaluate the cell's culture's ability of scaffold for bone tissue engineering. Beta TCP scaffold fabricated using 3-D printing technology is evaluated for its biological properties for human osteoblast cell culture and proliferation assessment. Images acquired after 24, 48 and 72 hrs using optical microscopy confirmed cell proliferation and adhesion in the locality of scaffold. SEM images demonstrated that scaffold had high level of micro porosity, coarseness, appropriate pore interconnectivity and that osteoblast cell well nurtured within the scaffold. Cytotoxicity of the scaffold was analyzed by MTS assay. There was a remarkable distinction for cells exposed to beta TCP and positive control which proves no effect of scaffold on cell viability (Santos et al., 2012).

Bio-metal scaffold fabricated by selective laser sintering and its *in-vitro* cell culture studies using human osteosarcoma cells derived from bone are reported. Titanium powder mixed with silica sol in a ratio of 2:1 weight percent was used to fabricate hollow shell structures of bone scaffold. To analyze the scaffold biocompatibility sintered as well as a green part sample was tested using microculture tetrazolium test (MTT) assay. The optical density value, i.e. the number of live cells increased with cell culture time for sintered sample than the green part (Liu et al., 2013).

Scaffold fabricated through rapid prototyping technology has also proven its superiority in cell culture abilities than conventional approaches. Cell proliferation ability of scaffold fabricated by salt leaching and MSTL using PPF as a biodegradable material using MC3T3-E1 pre-osteoblast cells showed superior results for cell adhesion and cell proliferation for scaffold fabricated using MSTL, though the porosity for scaffold fabricated using MSTL

was lower i.e. 69.6 % as that of salt leached approach with a porosity level of 76.6 % (Lee, Ahn, Kim, & Cho, 2010). In another study cell response on scaffold fabricated by 3D plotter with that of salt leached scaffold is compared using PCL material. Both the scaffolds were fabricated with same size, i.e. (10 mm x 10 mm x 5 mm). A 3-D biplotter PCL scaffold was fabricated with nozzle diameter of 330 μm and a strand distance of 700 μm . Chondrocytes extracted from articular cartilage of porcine were seeded on both the types of scaffolds. After 8 weeks of incubation it was observed that chondrocytes started filling up the interconnected pores and were fully spread on the 3D plotted scaffold surface. It was concluded that 3D plotted scaffold supports the speedy tissue formation with cell attachment in short time (Hee et al., 2010). Demonstration of different cell sources that are currently used in bone tissue regeneration is shown on Table 2.

Table 2. Cell currently used in bone tissue engineering

Cell Source	Cell Type	Features	Limitations	References
Stem Cells (Adult)	Bone marrow derived mesenchymal stem cells	Less immunogenic Differentiate into osteogenic lineage	Inadequate efficiency	Mafi et al., 2011
	Periosteal tissue derived mesenchymal cells	Better mineralization and neovascularization	Less supply	Salgado, Olga, & Rui, 2004
	Adipose tissue derived mesenchymal cells	Responds to osteogenic induction and differentiate to osteoblast	Low efficiency	Zu k et al., 2001
	Dental tissue derived progenitor cells (Ectomesenchymal cells)	Capable of differentiating into cartilage, bone and ligaments cells	Less supply	Su, Wu, & Huang, 2014
Stem Cell (Embryonic)	Blastocyst derived stem cells	Pluripotent cells	Prone to genetic alterations	Marolta et al., 2012
Stem cells (Fetal)	Umbilical cord derived stem cells	Multipotent with high proliferative capability	Less supply	Seong et al., 2010
	Cord blood derived stem cells	High potential, good efficiency	Autograft non-accessibility	Ribeiro et al., 2013
	Amniotic fluid derived stem cells	Differentiate into osteoblast. Formation of interconnected network for communication and transport between osteocyte	Less supply	Ribeiro et al., 2013 Takahashi & Yamanaka, 2006
Tissue specific	Osteoblastic cells		Less resource	
Genetically modified osteogenic cells	Adenoviral BMP (In Vivo delivery, gene construct)	Bone formation in subcutaneous and intramuscular ectopic sites	Host immune and inflammation	Hutmacher & Garcia, 2005
	Retroviral-BMP transduced osteogenic cells (Ex Vivo gene delivery)	Demonstrate bone regeneration in ectopic sites.	Immunosuppressant therapy	Tsuchida et al., 2003
	Induced pluripotent stem cells (iPS)	Generation of patient specific tissue	Low yield, Inefficient and costly	Takahashi & Yamanaka, 2006

4.2. in-vitro Culture Systems

Static cell culture condition is widely used in the field of tissue engineering for preliminary studies. Use of dynamic cell culture is more comparable to in-vivo conditions as compared to the static cell culture system. Bioreactors provide the 3D dynamic and mechanical in vivo body environment. They are designed to provide all necessary nutrients and biological cues to the cells seeded deep within a scaffold for its survival, proliferation and differentiation to produce extracellular matrix (Sladkova & Maria de Peppo, 2014). It has been seen in a study that extracellular matrix (ECM) gets uniformly distributed in 3D scaffold by using flow perfusion bioreactor after the period of 16 days in comparison to static condition in the presence of osteogenic cells (Zhang et al., 2010). Some popular bioreactors used in the field of bone tissue engineering areas:

4.2.1 Spinner Flask Bioreactor

It is a simple bioreactor, devised to provide convective flow so that hydrodynamic forces are produced to enhance mass transfer. A spinner flask director can accommodate large number of scaffolds, but the utility is limited for the reconstruction of flat bones or for bone patches (Rauh, Milan, Gunther, & Stiehler, 2011).

4.2.2 Rotating Wall Vessels

It consists of rotating concentric cylinders filled with culture medium where oxygen in media is provided via a coaxial tubular silicon membrane. Botchwey et al. (2004) on culturing SaOS-2 bone cells onto porous, three-dimensional degradable poly (lactic-co-glycolic acid) scaffold in a rotating wall vessel bioreactor demonstrated that cells maintained an osteoblastic phenotype and showed a significant increase in alkaline phosphatase (ALP) activity and matrix mineralization compared to cells cultured under static conditions (Botchwey, Levine, Pollack, & Laurencin, 2004). However, its application is limited to small scaffold size as they fail to conduct optimal mass transport to the core (Rauh, Milan, Gunther, & Stiehler, 2011). When compared with spinner flask, on culturing rat MSCs, low secretion of osteocalcin than a spinner flask is observed. Though it solves a few of the limitation of static culture, but results from expression of osteoblastic markers are not adequate (Gasper, Gomide, & Monteiro, 2012).

4.2.3 Perfusion Flask Bioreactor

Perfusion systems are complex since they can perfuse fluid directly through the scaffold to ensure uniform mixing of media, which results in better mass transport inside the large constructs, and up regulate expression of osteoblastic markers. It consists of pump, culture media reservoir, tubing circuit and columns to hold the scaffold. Several studies reveal that flow perfusion in comparison with static culture shows increase in ALP activity as well as Osteopontin which are expressed after differentiation of MSCs (Cartmell et al., 2003). Zhang et al. (2010) demonstrated differentiation of cells, leading to increase in ALP activity and calcium mineralization when human fetal MSCs seeded onto PCL/ β -Tricalcium phosphate block cultured using perfusion flask. Both in vitro and in vivo results showed proliferation and ectopic bone calcification respectively in mice (Zhang et al., 2010). Also, BM-MSCs seeded on poly (lactic -co-glycolic acid) /PCL cylindrical scaffold cultured in perfusion flask for 10 days prior to implantation in the femoral condyle of nude mice shows increase bone formation when compared with static culture (Sladkova & Maria de Peppo, 2014).

5. Animal Studies (in-vivo)

It is of prime importance to evaluate the performance of engineered tissue construct on various preclinical approaches before implantation in humans. The first phase includes preclinical trials on smaller animals in order to assess the given concept. After the acquisition of positive results, studies are extended to trials on larger animals (Salgado, Olga, & Rui, 2004). It is necessary to evaluate the performance of the construct which is comparable to the physiological response in humans. The success of preclinical studies depends upon the choice of animal model to access the viability of determining tissue engineering concept. The two most important properties to be considered when choosing the animal model is:

- 1) It must be comparable biologically and identifiable to human physiology.
- 2) The bone defect under study must fail if not treated with the TE approach under study (Goldstein, 2002).

If the aim of the study is to evaluate the porosity and permeability of fabricated tissue engineered scaffold for tissue growth and proliferation, then simple ectopic models can be considered very good (Pearce et al., 2007). Also for such studies subcutaneous models like rats can be considered where the scaffold is implanted into the back of the animal or other ectopic sites like peritoneal cavity. This approach can be considered to study osteoconductivity and bone formation when the scaffold is seeded with cells and growth factor supplemented with osteodifferentiation medium. Immunogenic response in such animals is a limitation which can be overcome by using athymic nude mice when the xenogeneic cell source is used (Viateau et al., 2008). Polylactic acid coated polyglycolic acid (PLA/PGA) scaffold and HA/PCL scaffold was fabricated to restore goat femoral head. The scaffolds were fabricated in two parts, i.e. Cartilage regeneration of femora condyle and bone regeneration of the femoral condyle. The surface morphology of femoral head of the goat, with and without cartilage was acquired by laser scanning to get the 3D model of articular cartilage. Resin model of PLA/PGA scaffold with 10 % PLA content was fabricated using 3D printing. The scaffold was molded to define the anatomical profile of the articular surface. Scaffold for bone generation of femoral condyle was fabricated using HA/PCL. 40 weight % HA powder was mixed with 60 weight % PCL pellets in slurry at 120° c and the scaffold was fabricated using FDM technology. Chondrocytes extracted from the cartilage samples of the femoral compartment of the knee joint were seeded on the PLA / PEG scaffold for cartilage regeneration. Similarly BMSCs extracted from the tibial condyle were seeded on the HA / PCL scaffold for femoral condyle bone regeneration. Together, PLA/PGA scaffold for upper cartilaginous part and HA/PCL scaffold for the osseous part were implanted in dorsum of athymic nude mice subcutaneously for 10 weeks. After 10 weeks of in-vivo implantation the structure retained its shape with unbroken cartilage like surface. At the cross-section 1.5 mm thick cartilage layer was observed on the surface of the femoral head and firm bone tissue were filled in the macro channels of scaffold (Ding et al., 2013).

The popularly used animal to study bone defects are rabbits, dogs, rats and sheep. The tissue engineered construct under a load bearing condition can be studied on the femur bone of rabbits (Salgado, Olga, & Rui, 2004). However pig and sheep models are used scarcely because of high cost. Histological staining methodologies are popular to observe the bone union at the two osteotomies like callus formation, new bone formation, resorption of the bone graft, marrow changes and cortex remodeling in in-vivo assays (Muschler et al., 2010). Computerized image and radiographic analysis make possible to observe penetration of bone tissue, thickness of non - mineralized bone tissue, surfaces covered by osteoblast, area of trabeculae, area of vascular tissue, and void space (Viateau et al., 2008). PLLA/TCP scaffold fabricated using (LDM) low temperature deposition manufacturing was used to heal 20 mm segmental defect in canine radiuses of 20 skeletally mature beagle dogs. The approximate weights of dogs were 10 to 14 kg. The scaffold was fabricated layer by layer in X and Y direction to make hollow cylindrical structure with external and internal diameter of 10 and 5mm respectively. Bovine bone morphogenic protein (bBMP) extracted from bovine diaphyseal bone were loaded on the scaffold and was implanted in the defect site. X-ray images revealed that there was a complete bone formation after 24 weeks of implantation. Also, no chronic lymphocytic infiltrates or giant cell formation was observed in any part, which concluded that implanted scaffold is biocompatible (Xiong et al., 2002).

Octacalcium phosphate (OCP) scaffold fabricated using 3D printing to repair designed cranial bone defect on 5 rabbits were investigated by Komlev. et.al., 2015. Scaffold with 20 mm diameter with 16 holes of 1 mm diameter was printed using custom designed 3D printer. The printed scaffold was placed in the center of the calvaria from the occipital to the frontal bone to mark the defect edges. Defects were made and scaffolds were implanted and the injuries were closed by intermittent sutures. All the rabbits were sacrificed after 6.5 months and calvaria from each bone defect area was removed. Computed tomography scans showed that the circumferential area of implanted material was fully incorporated with surrounding tissue (Komlev et al., 2015). Table 3 shows the in-vitro and in-vivo studies of 3D printed scaffolds.

Table 3. In vitro and in vivo studies of 3D printed scaffolds.

Biomaterial	Technique	Architecture	Cells source	In Vitro	Animals	In Vivo	Ref
Hydroxyapatite (HA)	3D Printing	Channel structures with inclined layers of 45° & diameters of about 500 μ m	MC3T3-E1 Mice fibroblasts	The cells showed Good attachment and proliferation into the HA matrices.	-	-	Leukers et al., 2005
Ti6Al4V	3D Bioplotter	Cylinder with central hole (intramuscular implantation)	BMSCs from iliac crest	-	Dutch milk goats	Bone formation observed between Six to ninth week of Implantation.	Li et al., 2007b
Ti6Al4V	3D Bioplotter	Block with inner hole (orthotopic implantation)	BMSCs from iliac crest	-	Dutch milk goats	The bone formation started before third week of Implantation.	Li et al., 2007a
PCL	3D Bioplotter	Basic, basic-off set, crossed and crossed offset	BMSCs from male Sprague Dawley rats.	Higher cell proliferation after 7, 14 & 21 days	-	-	Yilgor et al., 2008
PPF	MSTL	Block with different pores	MC3T3-E1	Best cell proliferation were seen in 350 μ m and worst in 500 μ m	-	-	Lee, et al., 2010
PLGA/T CP	LDM	Patient specific alveolar bone architecture obtained by Computed tomography.	Human BMSCs	Attachment and proliferation of cell confirmed after 7-8 days	-	-	Li et al., 2011
PCL PCL/TCP	SLS	Cylinder for Tibial defect	-	-	Mountain sheep	X rays showed	Lohfeld et al., 2012

						the formation of weak mineralized Callus	
PCL/HA	3D printing	Femoral condyle	BMSCs of goat	-	Athymic nude mice	Cuboidal osteoblast like cells and osteocytes seen on surface of new Bone	Ding et al., 2013
HA/PELA	F D M		NIH3T3 fibroblasts	Osteogenic differentiation after Culture induction and produce mineralized extracellular matrix.	-	-	Kutikov, Gurijala, & Song, 2014
Bioactive glass-ceramic scaffold.	Laser Rapid Prototypi-ng	Cubic block of size 10mm x 10mm x 10mm with square hole of size 1mm.	0.3 g of bioactive Glass ceramic scaffolds were immersed into 200 ml of SBF.	Hydroxycarbon ate apatite crystals formed in 14 days.			Li et al., 2013
PLLA + T CP	LDM	Hollow cylindrical structure with square strands in X & Y direction.	Bovine bone morphogenic protien (bBMP) from bovine diaphyseal bone	Beagle dogs.	Radiographic images confirmed complete bone regeneration after 24 weeks.		Xiong et al., 2002
Beta T CP	3D-Printing	Solid cylindrical Beta T CP scaffold with diameter and length of 10mm and 20mm resp.	Human Osteoblast cells	Cell adhesion And proliferation in the surroundingarea of Beta -T CP scaffold. Also, no acute cytotoxicity effect is seen in Beta -T CP Scaffold.			Santos et al., 2012
(Titanium + Silica solution) slurry	SLS	Hollow shell structure of tibia bone.	Human osteogenic sarcom (MG63)	OD (Optical density) value increased with cell culture time			Liu et al., 2013

6. Future Scope

Demand for processes such as 3DP will increase in the coming years due to their ability to make custom medical devices that can be tailored for patient specific and defect specific clinical needs. The most critical issue that needs consideration is the mechanical properties of porous scaffolds. Raising the porosity will decline the strength of the scaffolds. Low strength makes these scaffolds brittle and difficult to handle. Use of biodegradable polymer infiltration to enhance strength and toughness in these scaffolds is one way to minimize this problem. Various challenges still remain with the design of scaffold for specific cell types as needed for guided tissue regeneration. A new generation of scaffolds is also needed, with appropriate porosity, degradation rates, and mechanical properties. Also printing live cells or adding growth factors/drugs is another important area for research. Another approach can be surface modification, such as the coating of the scaffolds. Liu and Ma. (2004) have shown that by doing so it is possible to direct cells to a more osteogenic phenotype (Liu & Ma, 2004). However, most of the challenges are restricted to the viability of the cells, growth factors and drugs after printing. Although an existing technique is to build structures with parallel composition to that of tissue, still we are a long way from complete printing functioning tissue. Optimization of process & property, in vitro and in vivo research are desirable to make any of those approaches useful toward bone tissue engineering.

Acknowledgements

The authors declare that they have no conflict of interest. Financial disclosure: This research was not supported by any funding organization.

References

- Aust, L., Cooper, L., Devlin, B., Laney, T., Foster, G., Halvorsen, Y. D. C., ... Wilkison, W. O. (2004). Adipose tissue-derived adult stem cell: Potential for cell therapy. *Stem cell therapy for autoimmune diseases* (Chapter 5, pp. 24-30).
- Bose, S., Vahabzadeh, S., & Bandyopadhyay, A. (2013). Bone tissue engineering using 3D printing. *Material Today*, 16(12), 496-504. <http://dx.doi.org/10.1016/j.mattod.2013.11.017>
- Botchwey E. A., Levine, E. M., Pollack, S. R., & Laurencin, C. T. (2004). Bioreactor-based bone tissue engineering: The influence of dynamic flow on osteoblast phenotypic expression and matrix mineralization. *Proc Natl Acad Sci U S A*, 101(31), 11203-11208. <http://dx.doi.org/10.1073/pnas.0402532101>
- Caetano, G. F., Bartolo, P. J., Domingos, M., Oliveira, C. C., Leite, M. N., & Frade, M. A. C. (2015). Osteogenic differentiation of adipose-derived mesenchymal stem cells into Polycaprolactone (PCL) scaffold. *Procedia Engineering*, 110, 59-66. <http://dx.doi.org/10.1016/j.proeng.2015.07.010>
- Cai, S., & Xi, J. (2008). A control approach for pore size distribution in the bone scaffold based on the hexahedral mesh refinement. *Computer-Aided Design*, 40, 1040-1050. <http://dx.doi.org/10.1016/j.cad.2008.09.004>
- Cartmell, S. H., Porter, B. D., Garcia, A. J., & Guldberg, R. E. (2003). Effects of Medium Perfusion Rate on Cell-Seeded three-Dimensional Bone Construct in Vitro. *Tissue Engineering*, 9(6), 1197-1203. <http://dx.doi.org/10.1089/10763270360728107>
- Chen, Z., Li, D., Lu, B., Tang, Y., Sun, M., & Xu, S. (2005). Fabrication of osteo-structure analogous scaffolds via fused deposition modeling. *Scripta Materialia*, 52, 157-161. <http://dx.doi.org/10.1016/j.scriptamat.2004.08.006>
- Chua, C. K., Leong, K. F., Cheah, C. M., & Chua, S. W. (2003a). Development of a Tissue Engineering Scaffold Structure Library for Rapid Prototyping. Part 1: Investigation and Classification. *Int J Adv Manuf Technol*, 21, 291-301.
- Chua, C. K., Leong, K. F., Cheah, C. M., & Chua, S. W. (2003b). Development of a Tissue Engineering Scaffold Structure Library for Rapid Prototyping Part 2: Parametric Library and Assembly Program. *Int Adv Manuf Technol*, 21, 302-312.
- Colnot, C. (2011). Cell Sources for Bone Tissue Engineering: Insights from Basic Science. *Tissue Engineering. Part B, Reviews*, 17(6), 449-457. <http://dx.doi.org/10.1089/ten.TEB.2011.0243>
- Ding, C., Qiao, Z., Jiang, W., Li, H., Wei, J., Zhou, G., & Dai, K. (2013). Regeneration of a goat femoral head using a tissue-specific, biphasic scaffold fabricated with CAD/CAM technology. *Biomaterials*, 34, 6706-6716. <http://dx.doi.org/10.1016/j.biomaterials.2013.05.038>
- Fedorovich, N. E., Alblas, J., Hennink, W. E., Oner, F. C., & Dhert, W. J. A., (2011). Organ printing: the future of bone regeneration. *Trends in Biotechnology*, 29(12), 601-606. <http://dx.doi.org/10.1016/j.tibtech.2011.07.001>
- Gasper, D. A., Gomide, V., & Monteiro, F. J. (2012). The role of perfusion bioreactor in bone tissue engineering. *Biomatter*, 2(4), 167-175. <http://dx.doi.org/10.4161/biom.22170>
- Goldstein, S. A. (2002). Tissue engineering: functional assessment and clinical outcome. *Ann NY Acad Sci*, 1(961), 183-192.
- Hass, R., Kasper, C., Böhm, S., & Jacobs, R. (2011). Different populations and sources of human mesenchymal stem cells (MSC): A comparison of adult and neonatal tissue-derived MSC. *Cell Communication and Signaling*, 9(12). <http://dx.doi.org/10.1186/1478-811X-9-12>
- Hee, L. J., Su-A, P., KoEun, P., Jae-Hyun, K., Shik, K. K., Jihye, L., & WanDoo, K. (2010). Fabrication and characterization of 3D scaffold using 3D plotting system. *Bionic Engineering*, 55(1), 94-98. <http://dx.doi.org/10.1007/s11434-009-0271-7>
- Hutmacher, D. W., & Garcia, A. J. (2005). Scaffold-based bone engineering by using genetically modified cells. *Gene*, 347(1), 1-10. <http://dx.doi.org/10.1016/j.gene.2004.12.040>

- Hutmacher, D. W., Sittering, M., & Risbud, M. V. (2004). Scaffold-based tissue engineering: rationale for computer-aided design and solid free-form fabrication systems. *TRENDS in Biotechnology*, 22(7), 354-362. <http://dx.doi.org/10.1016/j.tibtech.2004.05.005>
- Kalita, S. J., Bose, S., Hosick, H. L., & Bandyopadhyay, A. (2003). Development of controlled porosity polymer-ceramic composite scaffolds via fused deposition modeling. *Materials Science and Engineering C*, 23, 611-620. [http://dx.doi.org/10.1016/S0928-4931\(03\)00052-3](http://dx.doi.org/10.1016/S0928-4931(03)00052-3)
- Karageorgiou, V., & Kaplan, D. (2005). Porosity of 3D biomaterial scaffolds and osteogenesis. *Biomaterials*, 26, 5474-5491. <http://dx.doi.org/10.1016/j.biomaterials.2005.02.002>
- Komlev, V. S., Popov, V. K., Mironov, A. V., Fedotov, A. Y., Teterina, A. Y., Smirnov, I. V., ... & Deev, R. V. (2015). 3D printing of octacalcium phosphate bone substitutes. *Frontiers in bioengineering and biotechnology*, 3. <http://dx.doi.org/10.3389/fbioe.2015.00081>
- Kutikov, A. B., Gurijala, A., & Song, J. (2014). Rapid Prototyping Amphiphilic Polymer/ Hydroxyapatite Composite Scaffolds with Hydration-Induced Self-Fixation Behavior. *Tissue Engineering: Part C*, 21(3), 229-241. <http://dx.doi.org/10.1089/ten.TEC.2014.0213>
- Landers, R., Pfister, A., Hubner, U., John, H., Schmelzeisen, R., & Mulhaupt, R. (2002). Fabrication of soft tissue engineering scaffolds by means of rapid prototyping techniques. *Journal of material science*, 37, 3107-3116.
- Lee, J. W., Ahn, G., Kim, J.Y., & Cho, D.W. (2010). Evaluating cell proliferation based on internal pore size and 3D scaffold architecture fabricated using solid freeform fabrication technology. *J Mater Sci: Mater Med*, 21, 3195-3205. <http://dx.doi.org/10.1007/s10856-010-4173-7>
- Leukers, B., Gulkan, H., Irsen, S. H., Milz, S., Tille, C., Schieker, M., & Seitz, H. (2005). Hydroxyapatite scaffolds for bone tissue engineering made by 3D printing. *Journal of Materials Science: Materials in Medicine*, 16(12), 1121-1124. <http://dx.doi.org/10.1007/s10856-005-4716-5>
- Levi, B., & Longaker, M. T. (2011). Adipose derived stromal cells for skeletal regenerative medicine. *Stem Cells*, 29, 576. <http://dx.doi.org/10.1002/stem.612>
- Li, H., Yang, J. Y., Su, P. C., & Wang, W. S. (2012). Computer aided modeling and pore distribution of bionic porous bone structure. *Journal of Central South University*, 19, 3492-3499. <http://dx.doi.org/10.1007/s11771-012-1434-2>
- Li, J. P., Habobovic, P., Doel, M., Wilson, C. E., Wijn, J. R., Blitterswijk, C. A., ... Groot, K. (2007). Bone ingrowth in porous titanium implants produced by 3D fiber deposition. *Biomaterials*, 28, 2810-2820. <http://dx.doi.org/10.1016/j.biomaterials.2007.02.020>
- Li, J., Wijn, J. R., Blitterswijk, C.A.V., & Groot, K.D. (2006a). Porous Ti6Al4V scaffold directly fabricating by rapid prototyping: Preparation and in vitro experiment. *Bio materials*, 27, 1223-1235. <http://dx.doi.org/10.1016/j.biomaterials.2005.08.033>
- Li, J., Habibovic, P., Yuan, H., Doel, M., Wilson, C.E., Wijn, J. R., Blitterswijk, C. A., & Groot, K. (2007b). Biological performance in goats of a porous titanium alloy-biphasic calcium phosphate composite. *Biomaterials*, 28, 4209-4218. <http://dx.doi.org/10.1016/j.biomaterials.2007.05.042>
- Li, J., Zhang, L., Lv, S., Li, S., Wang, N., & Zhang, Z. (2011). Fabrication of individual scaffolds based on a patient-specific alveolar bone defect model. *Journal of Biotechnology*, 151, 87-93. <http://dx.doi.org/10.1016/j.jbiotec.2010.10.080>
- Li, Z., Chen, X., Zhao, N., Dong, H., Li, Y., & Lin, C. (2013). Stiff macro-porous bioactive glass - ceramic scaffold: Fabrication by rapid prototyping template, characterization and in vitro bioactivity. *Material Chemistry and Physics*, 141, 76-80. <http://dx.doi.org/10.1016/j.matchemphys.2013.05.001>
- Lian, X., Bao, X., Al-Ah mad, A., Liu, J., Wu, Y., Dong, W., ... Palecek, S. P. (2014). Efficient differentiation of human pluripotent stem cells to endothelial progenitors via small-molecule activation of WNT signaling. *Stem Cell Reports*, 3, 804-816. <http://dx.doi.org/10.1016/j.stemcr.2014.09.005>
- Lin, L., Huang, X., Hu, Q., & Fang, M. (2006, November). Fabrication of tissue engineering scaffolds via rapid prototyping machine. In *Technology and Innovation Conference, 2006. ITIC 2006. International* (pp. 1280-1285). IET.
- Liu, F. H. (2012). Synthesis of bioceramic scaffolds for bone tissue engineering by rapid prototyping technique. *J Sol-Gel Sci Technol*, 64, 704-710. <http://dx.doi.org/10.1007/s10971-012-2905-5>

- Liu, F. H., Lee, R.T., Lin, W. H., & Liao, Y. S. (2013). Selective laser sintering of bio-metal scaffold. *Procedia CIRP*, 5, 83-87.
- Liu, X., & Ma, P. X., (2004). Polymeric Scaffolds for Bone Tissue Engineering. *Annals of Biomedical Engineering*, 32(3), 477-486. <http://dx.doi.org/10.1023/B:ABME.0000017544.36001.8e>
- Liulan, L., Qing xi, H., Xianxu, H., & Gaochun, X. (2007). Design and Fabrication of Bone Tissue Engineering Scaffolds via Rapid Prototyping and CAD. *Journal of rare earth*, 25, 379-383.
- Locke, M., Windsor, J., & Dunbar, P. R. (2008). Human adipose - derived stem cells: isolation, characterization and applications in surgery. *ANZJ Surg*, 79, 235-244. <http://dx.doi.org/10.1111/j.1445-2197.2009.04852.x>
- Lohfeld, S., Cahill, S., Barron, V., McHugh, P., Dürselen, L., Kreja, L., ... Ignatius, A. (2012). Fabrication Mechanical and In Vivo Performance of Polycaprolactone /Tricalciumphosphate Composite Scaffold. *Biomaterialia*, 8, 3446-3456. <http://dx.doi.org/10.1016/j.actbio.2012.05.018>
- Mafi, R., Hindocha, S., Mafi, P., Griffin, M., & Khan, W. S. (2011). Sources of adult mesenchymal stem cells applicable for musculoskeletal applications - a systematic review of the literature. *The Open Orthopedics Journal*, 5, 242-248. <http://dx.doi.org/10.2174/1874325001105010242>
- Maleksaedi, S., Wang, J. K., Hajje, A.E., Harb, L., Guneta, V., He, Z., ... Ruys, A.J. (2013). Towards 3D printed bioactive titanium scaffolds with bimodal pore size distribution for bone in growth. *Procedia CIRP*, 5, 158-163. <http://dx.doi.org/10.1016/j.procir.2013.01.032>
- Marolta, D., Camposa, I. M., Bhu miratanaa, S., Korena, A., Petridisa P., Zhang, G., ... Novakovica, G. V. (2012). Engineering bone tissue from human embryonic stem cells. *PNAS*, 109(22), 8705-8709. <http://dx.doi.org/10.1073/pnas.1201830109>
- Marolta, D., Camposa, I. M., Bhu miratanaa, S., Korena, A., Petridisa P., Zhang, G., ... Novakovica, G. V. (2012). Engineering bone tissue from human embryonic stem cells. *PNAS*, 109(22), 8705-8709. <http://dx.doi.org/10.1073/pnas.1201830109>
- Melchels, F. P., Tonnarelli, B., Olivares, A. L., Martin, I., Lacroix, D., Feijen, J., ... & Grijpma, D. W. (2011). The influence of the scaffold design on the distribution of adhering cells after perfusion cell seeding. *Biomaterials*, 32(11), 2878-2884. <http://dx.doi.org/10.1016/j.biomaterials.2011.01.023>
- Mourino, V., & Boccaccini, A. R. (2010). Bone tissue engineering therapeutics: controlled drug delivery in three-dimensional scaffolds. *J. R. Soc. Interface*, 7, 209-227. <http://dx.doi.org/10.1098/rsif.2009.0379>
- Muschler, G. F., Raut, V. P., Patterson, T. E., Wenke, J. C., & Hollinger, J. O. (2010). The design and use of animal models for translational research in bone tissue engineering and regenerative medicine. *Tissue Eng Part B Rev*, 16(1), 123-145. <http://dx.doi.org/10.1089/ten.TEB.2009.0658>
- Pearce, A. I., Richards, R.G., Milz, S., Schneider, E., & Pearce, S. G. (2007). Animal Models for Implant Bio material Research in Bone: A Review. *European Cells and Materials*, 13, 1-10.
- Podshivalov, L., Gomes, C.M., Zocca, A., Guenster, J., Yoseph, P. B., & Fischer, A. (2013). Design, analysis and additive manufacturing of porous structures for Biocompatible micro-scale scaffolds. *CIRP Conference on Bio manufacturing, Procedia CIRP* 5, 247-252. <http://dx.doi.org/10.1016/j.procir.2013.01.049>
- Rainer, A. M., Accota, D., Porcellinis, S. D., Guglielmelli, E., & Trombetta, M. (2011). Load adaptive scaffold architecturing: A Bioinspired Approach to the design of porous additively manufactured scaffolds with optimized mechanical properties. *Annals of Biomedical Engineering*, 40(4). <http://dx.doi.org/10.1007/s10439-011-0465-4>
- Rauh, J., Milan, F., Gunther, K., & Stiehler, M. (2011). Bioreactor Systems for Bone Tissue Engineering. *Tissue Engineering: Part B*, 17(4), 263-280. <http://dx.doi.org/10.1089/ten.teb.2010.0612>
- Ribeiro, A., Laranjeira, P., Mendes, S., Velada, I., Leite, C., Andrade, P., & Paiva, A. (2013). Mesenchymal stem cells from umbilical cord matrix, adipose tissue and bone marrow exhibit different capability to suppress peripheral blood B, natural killer and T cells. *Stem Cell Research & Therapy*, 4(5). <http://dx.doi.org/10.1186/scrt336>
- Sachlos, E., & Czernuszka, J. T. (2003). Making Tissue Engineering scaffold work. Review on the application of solid freeform fabrication technology to the production of Tissue Engineering Scaffolds. *European cells and materials*, 5, 29-40.

- Saito, E., Kang, H., Taboas, J. M., Diggs, A., Flanagan, C. L., & Hollister, S. J. (2010). Experimental and computational characterization of designed and fabricated 50:50 PLGA porous scaffolds for human trabecular bone applications. *J Mater Sci: Mater Med*, *21*, 2371-2383. <http://dx.doi.org/10.1007/s10856-010-4091-8>
- Salgado, A. J., Olga, P. C., & Rui, L. R. (2004). Bone Tissue Engineering: State of the Art and Future Trends. *Macromol. Biosci.*, *4*, 743-765. <http://dx.doi.org/10.1002/mabi.200400026>
- Santos, F. L. C., Silva, A. P., Lopes, L., Pires, I., & Correia, J. I. (2012). Design and production of sintered β -tricalcium phosphate 3D scaffolds for bone tissue regeneration. *Material science and engineering C*, *32*, 1293-1298. <http://dx.doi.org/10.1016/j.msec.2012.04.010>
- Seong, J. M., Kim, B. C., Park, J. H., Kwon, I. K., Mantalaris, A., & Hwang, Y. S. (2010). Stem cells in bone tissue engineering. *Biomed. Mater.*, *5*. <http://dx.doi.org/10.1088/1748-6041/5/6/062001>
- Serra, T., Planell, J. A., & Navarro, M. (2013). High-resolution PLA-based composite scaffolds via 3-D printing technology. *Acta Biomaterialia*, *9*, 5521-5530. <http://dx.doi.org/10.1016/j.actbio.2012.10.041>
- Sladkova, M., & Maria de Peppo, G. (2014). Bioreactor Systems for Human Bone Tissue Engineering. *Processes*, *2*, 494-525. <http://dx.doi.org/10.3390/pr2020494>
- Su, W., Wu, P., & Huang, T. (2014). Osteogenic differentiation of stem cells from human exfoliated deciduous teeth on poly (ϵ -caprolactone) nano fibers containing strontium phosphate. *Materials Science and Engineering: C*, *46*(1), 427-434. <http://dx.doi.org/10.1016/j.msec.2014.10.076>
- Sun, W., & Lal, P. (2000). Recent development on computer aided tissue engineering. *Computer Methods and Programs in Biomedicine*, *67*, 85-103.
- Sun, W., Starly, B., & Darling, N. A. (2005). Bio - CAD modeling and its applications in computer-aided tissue engineering. *Computer-Aided Design*, *37*, 1097-1114. <http://dx.doi.org/10.1016/j.cad.2005.02.002>
- Sun, W., Starly, B., Darling, A., & Gomez, C. (2004). Computer aided Tissue Engineering: application to biomimetic modeling and design of tissue scaffold. *Biotechnol. Appl. Biochem.*, *39*, 49-58.
- Takahashi, K., & Yamanaka, S. (2006). Induction of pluripotent stem cells from mouse embryonic and adult fibroblast cultures by defined factors. *Cell*, *126*(4), 663-676. <http://dx.doi.org/10.1016/j.cell.2006.07.024>
- Tsuchida, H., Hashimoto J., Crawford E., Manske P., & Lou J. (2003). Engineered allogeneic mesenchymal stem cells repair femoral segmental defect in rats. *J Orthop Res*, *21*(1), 44-53. [http://dx.doi.org/10.1016/S0736-0266\(02\)00108-0](http://dx.doi.org/10.1016/S0736-0266(02)00108-0)
- Viateau, V., Avramoglou, D. L., Guillemin, G., & Petite, H., (2008). Animal Models for Bone Tissue Engineering Purposes. *Sourcebook of Models for Biomedical Research*, 725-736.
- Wettergreen, M. A., Bucklen, B. S., Starly, B., Yuksel, E., Sun, W., & Liebschner, M. A. K. (2005). Creation of a unit block library of architectures for use in assembled scaffold engineering. *Computer-Aided Design*, *37*, 1141-1149. <http://dx.doi.org/10.1016/j.cad.2005.02.005>
- Williams, J. M., Adewunmi, A., Schek, R. M., Flanagan, C. L., Krebsbach, P. H., Feinberg, S. E., Hollister, S. J., & Das, S. (2005). Bone tissue engineering using polycaprolactone scaffolds fabricated via selective laser sintering. *Bio materials*, *26*, 4817- 4827. <http://dx.doi.org/10.1016/j.biomaterials.2004.11.057>
- Xiong, Z., Yan, Y., Wang, S., Zhang, R., & Zhang, C. (2002). Fabrication of porous scaffolds for bone tissue engineering via low-temperature deposition. *Scripta Materialia*, *46*, 771-776. [http://dx.doi.org/10.1016/S1359-6462\(02\)00071-4](http://dx.doi.org/10.1016/S1359-6462(02)00071-4)
- Xiong, Z., Yan, Y., Zhang, R., & Sun, L. (2001). Fabrication of porous poly (L-lactic acid) scaffolds for bone tissue engineering via precise extrusion. *Scripta Materialia*, *45*, 773-779. [http://dx.doi.org/10.1016/S1359-6462\(01\)01094-6](http://dx.doi.org/10.1016/S1359-6462(01)01094-6)
- Yan, X., Chen, X. B., & Bergstrom, D. J. (2011). Modeling of the flow within Scaffolds in Perfusion Bioreactors. *American Journal of Biomedical Engineering*, *1*(2), 72-77. <http://dx.doi.org/10.5923/j.ajbe.20110102.13>
- Yang, S., Leong, K. F., Du, Z., & Chua, C. K. (2001). The Design of Scaffolds for Use in Tissue Engineering. Part I. Traditional Factors. *Tissue Engineering*, *7*(6), 679-689.
- Yilgor, P., Sausa, R. A., Reis, R. L., Hasirci, N., & Hasirci, V. (2008). 3D Plotted PCL scaffold for Stem Cell Based Bone Tissue Engineering. *Macromol. Symp.*, *269*, 92-99. <http://dx.doi.org/10.1002/masy.200850911>

- Zein, I., Hutmacher, D. W., Tan, K. C., & Teoh, S. H. (2001). Fused deposition modeling of novel scaffold architectures for Tissue Engineering applications. *Bio materials*, *23*, 1169 -1185.
- Zhang, Z. Y., Teoh, S. H., Teo, E. Y., Chong, M. S. K., Shin, C. W., Tien, F. T., ... Chan, J. K.Y. (2010). A comparison of bioreactors for culture of fetal mesenchymal stem cells for bone tissue engineering. *Bio materials*, *31*, 8684-8695. <http://dx.doi.org/10.1016/j.biomaterials.2010.07.097>
- Zuk, P. A., Zhu, M., Mizuno, H., Futrell, J. W., Katz, A. J., Benhaim, P., ... Hedrick, M. H. (2001). Multilineage cells from human adipose tissue: implications for cell-based therapies. *Tissue Engineering*, *7*(2), 211–228. <http://dx.doi.org/10.1089/107632701300062859>

Copyrights

Copyright for this article is retained by the author(s), with first publication rights granted to the journal.

This is an open-access article distributed under the terms and conditions of the Creative Commons Attribution license (<http://creativecommons.org/licenses/by/4.0/>).